ACS OMEGA

http://pubs.acs.org/journal/acsodf

Article

Effects of Syngas Addition on Combustion Characteristics of Gasoline Surrogate Fuel

Qin Chen, Zhaolei Zheng,* and Ziji Zhu

Cite This: *ACS Omega* 2023, 8, 3929−3944

Read Online

ACCESS | Metrics & More | Article Recommendations

ABSTRACT: Syngas has the potential to become an alternative fuel for internal combustion engines. In this work, a detailed mechanism containing 1389 species and 5942 reactions was developed to examine the combustion of syngas/gasoline blends. The influence of syngas addition on the ignition delay time (IDT) and laminar flame speed of gasoline fuel was studied. Two influencing factors were considered: the mixing ratio of syngas and the H_2/CO ratio in syngas. The changes in heat release, free radical concentrations, and emissions were also studied. Syngas can boost the system's reaction activity and promote ignition in the high-temperature area over 1000 K. However, the diluting effect is visible at low temperatures below 1000 K, leading to an IDT lag. The effect of the H_2/CO ratio on the IDT was not as pronounced as expected. The addition of syngas can inhibit the knock combustion of the engine to a certain extent, but it will also lead to a violent exothermic process and a decrease in the total release of heat. Syngas addition increases the concentration of small molecule radicals and promotes the laminar flame speed. At higher temperatures and pressure levels, the trend of syngas/gasoline laminar flame speed is more dependent on changes in OH radical concentrations. The addition of syngas favors the promotion of complete combustion and the reduction of HC emissions but also results in an additional increase in CO. Combustion at lower temperatures has lower CO and HC emissions.

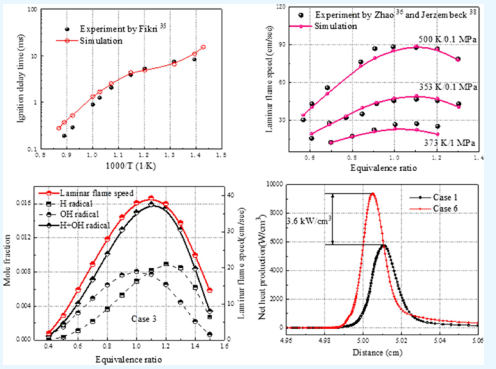

1. INTRODUCTION

In recent years, China's fast economic and social development has resulted in an increase in energy consumption and a greater reliance on fossil fuels, posing a threat to energy security.[1] On the other side, the country's large quantity of cars[2] has put a significant strain on the urban environment. Furthermore, stricter emission regulations[3] have been introduced. All these bring challenges to the development of cleaner fuels for internal combustion engines. Syngas contains a high percentage of hydrogen, which has the potential to become a hydrogen-rich fuel for internal combustion engines.

Syngas as an internal combustion engine fuel has been studied by many researchers. Although it performs well in combustion efficiency and emission,[4−6] syngas fuel can lead to a decrease in engine volumetric efficiency power when the synthetic gas fuel was fully used.[7] This may result in the output power and torque of the engine decrease by 20−40%.[8,9] Therefore, internal combustion engines are not suitable for using 100% syngas as fuel. Partial replacement of diesel or gasoline fuels with syngas can reduce fuel consumption and obtain lower power derating.[10] A blended fuel strategy using a mixture of fossil fuel and syngas has been studied by Ji et al.,[11,12] Singh and Mohapatra,[13] and Krishnamoorthi et al.[14] The addition of syngas can also help to improve the combustion efficiency and extend the lean burn limit.[8] Under certain conditions, the efficient and clean combustion can be achieved.[15,16] From the above studies, it was found that the application of syngas in dual fuel mode has more potential. Despite all the results obtained, more research and optimizations are still needed to achieve better combustion characteristics.

Chemical kinetic models of fuel are the basis for combustion process simulation studies. Reliable chemical kinetic models are particularly important for combustion and emission studies, as well as the optimization of combustion systems on engines. Syngas addition affects ignition delay time (IDT) and laminar flame speed, expanding the range of combustion equivalence ratios (ϕ) of fuel.[17] To be able to predict the performance of reformer gas (same as syngas, the latter are all called syngas) and *n*-heptane fuel blends in homogeneous charge compression ignition (HCCI) engines, Kongsereeparp and Checkel[18] and Neshat et al.[19] constructed mechanisms for fuel blends of syngas with *n*-heptane, respectively. And their results showed that the reformer gas delayed the ignition and combustion of the fuel in HCCI engines. Azimov et al.[20] constructed a dual fuel

Received: October 10, 2022
Accepted: December 20, 2022
Published: January 17, 2023

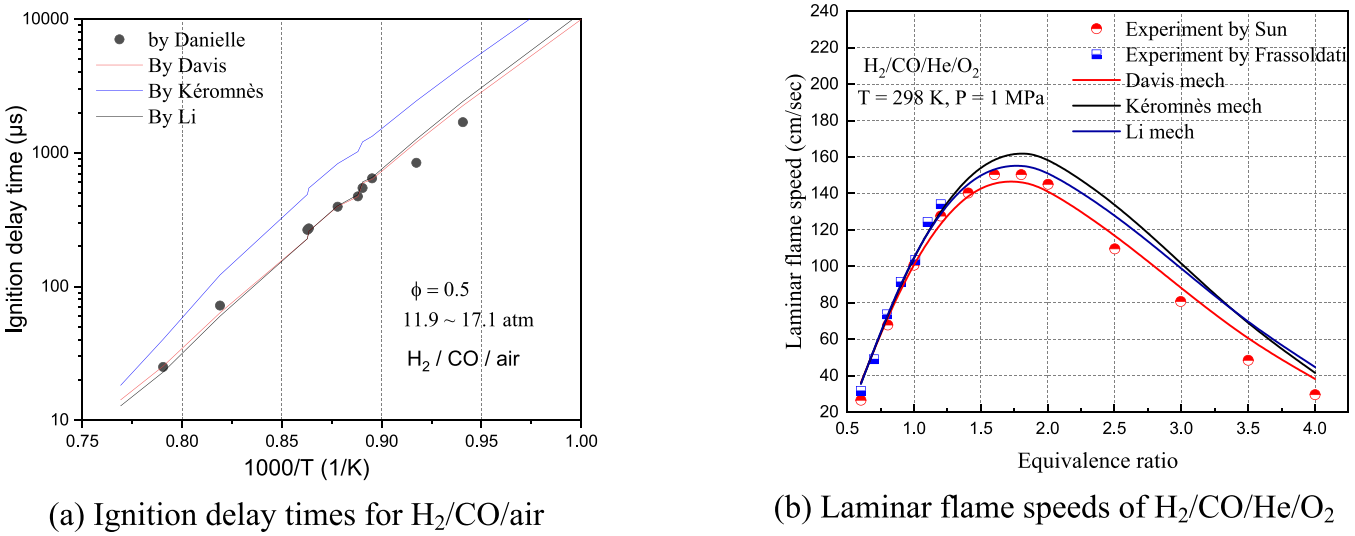

(a) Ignition delay times for H_2/CO/air (b) Laminar flame speeds of H_2/CO/He/O_2

Figure 1. (a and b) Comparison of predicted and experimental data. The ignition data measured by Kalitan and Petersen[31] at ϕ = 0.5 and pressures of 1.1−1.2 and 11.9−19.2 atm. The laminar flame speed data came from Sun et al.[32] and Frassoldati et al.[33] at 298 K, 1 MPa, H_2/CO = 1:1, and He/O_2 = 7:1.

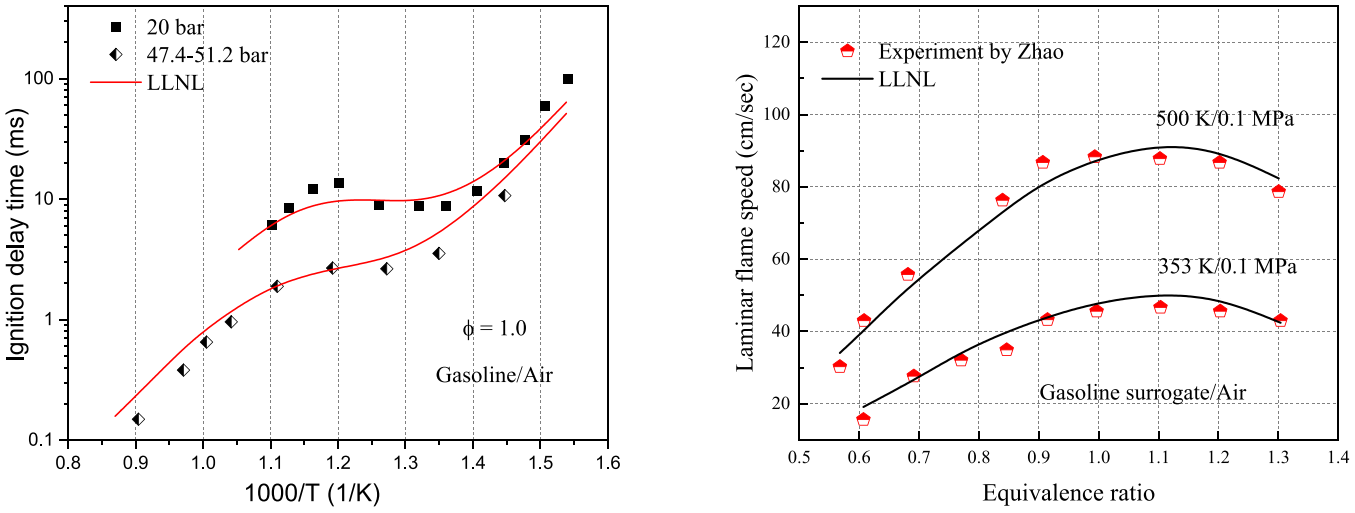

(a) Ignition delay times of gasoline/air (b) Laminar flame speeds of gasoline/air

Figure 2. (a and b) Validation of ignition delay time and laminar flame speed of the gasoline surrogate. The shock tube ignition data were measured by Fikri and co-workers.[35] The measurements of laminar flame speed came from Zhao et al.[36]

mechanism for *n*-heptane and syngas, and good prediction results were obtained in validation. Ra et al.[21] and Xu et al.[15] similarly constructed a dual-fuel chemical kinetic model with good prediction results for *n*-heptane and syngas and analyzed the effects of syngas addition on the reactivity controlled compression ignition (RCCI) engines. Jain et al.[17] and Kozlov et al.[22] proposed and validated the mechanism of syngas/isooctane hybrid fuels. The addition of syngas was found to have an impact on isooctane ignition, sensitivity reactions, and reaction paths. Neshat et al.[23,24] constructed a chemical kinetic model applicable to blended fuels with syngas and primary reference fuels (PRF, isooctane, and *n*-heptane). In the HCCI model, syngas addition affects the engine performance and emissions, as well as the peak of free radicals. The analysis based on the second law of thermodynamics is found to be also beneficial in controlling the irreversibility and heat transfer losses of the engine. By studying the effect of syngas addition on isooctane and *n*-heptane fuels in HCCI engines, Reyhanian and Hosseini[25] constructed a corresponding chemical kinetic model and found that the addition of syngas has a more significant chemical effect on *n*-heptane than on isooctane. Recent study came from Khan et al.[26] They investigated the effect of H_2, CO, and syngas addition on Haltermann gasoline. Two detailed chemical kinetic models were constructed for comparative analysis and included *n*-heptane, isooctane, toluene, and ethanol. At the Markstein length, H_2 led to instability, while CO enhanced the stabilization effect.

Although both *n*-heptane and isooctane are PRF and surrogates for gasoline, multicomponent surrogates that can better reflect the nature of fuels are hardly used. In addition, basic research on the effects of syngas addition on fuel combustion and emissions is still lacking. In this context, it is interesting to study the combustion behavior of syngas and multicomponent gasoline surrogate. The main objective of this

https://doi.org/10.1021/acsomega.2c06515
ACS Omega 2023, 8, 3929−3944

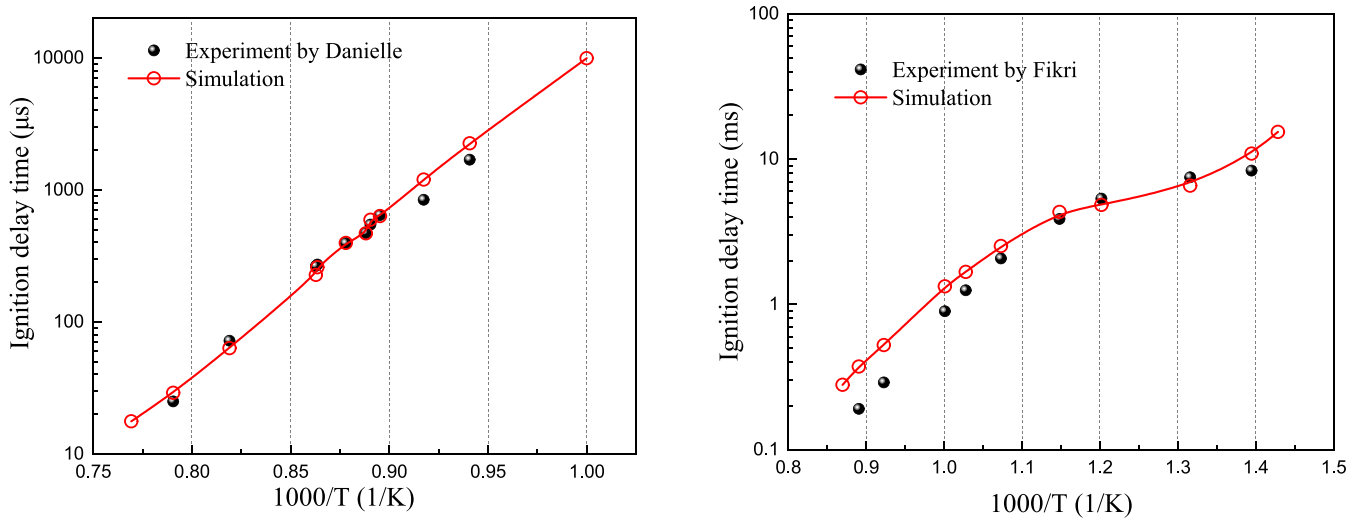

(a) H_2/CO/Air, ϕ = 0.5, P = 11.9~17.1 atm (b) Gasoline/Air, ϕ = 1.0, P = 29.9~33.1 bar

Figure 3. (a and b) Validation of ignition delay times of the syngas/gasoline mechanism.

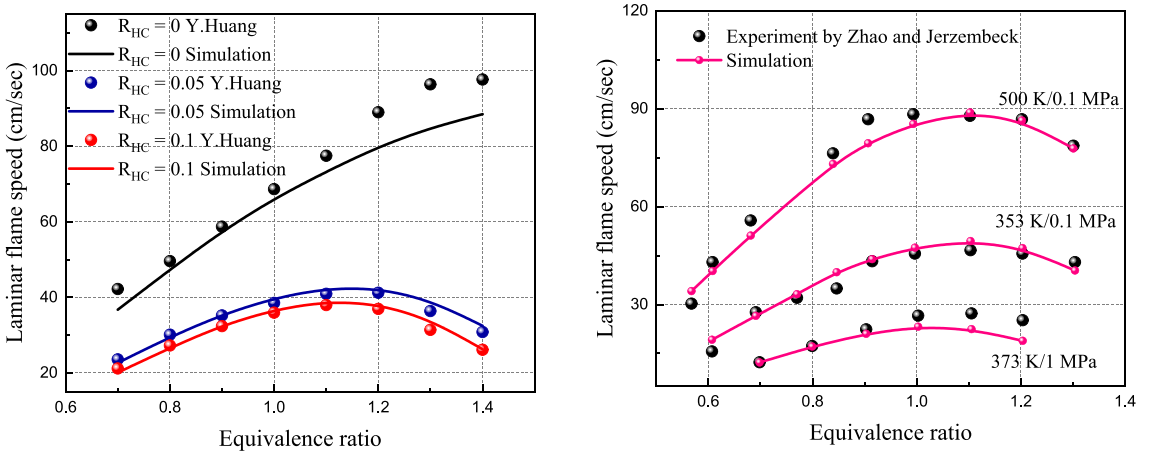

(a) Syngas/Isooctane/Air, T = 298 K, P = 0.1 MPa (b) Gasoline/Air, T = 353~500 K, P = 0.1~1 MPa

Figure 4. (a and b) Validation of laminar flame speeds of the syngas/gasoline mechanism.

paper is to develop a detailed chemical kinetic mechanism and to investigate the combustion behavior of a syngas/gasoline mixture under engine conditions. The model was verified using experimental data for syngas, gasoline, and syngas/isooctane. Based on this mechanism, the effects of the syngas blending ratio and internal H_2 ratio on the IDT, laminar flame speed, exothermic rate, small molecule concentration, and emissions were further investigated.

2. MECHANISM CONSTRUCTION AND VALIDATION

To simulate the effect of syngas addition on the IDT and laminar flame speed of gasoline fuel, numerical simulations were performed using the closed homogeneous reactor model and PREMIX code in Chemkin-Pro software. The starting point of the calculation was given by the initial temperature, pressure, syngas composition, and equivalence ratio (ϕ). During the simulations, the criterion of the ignition state when the maximum temperature gradient of the system temperature with time occurs was defined.[27]

The starting point of the research was the construction of the syngas/gasoline dual fuel mechanism. The chemical kinetic models of syngas constructed by Davis et al.,[28] Kéromnès et al.,[29] and Li et al.[30] were considered. Figure 1 compares the IDTs and laminar flame speeds of the three syngas mechanism predictions. The shock tube ignition data were measured by Kalitan and Petersen.[31] The experimental data of laminar flame speed came from Sun et al.[32] and Frassoldati et al.[33] as shown in Figure 1. From the reported results, the Davis mechanism was selected due to its better prediction accuracy.

Similarly, the mechanism of the LLNL gasoline surrogate developed by Mehl et al.[34] was also verified. The ignition data of gasoline were obtained from Fikri and co-workers[35] at an equivalence ratio (ϕ) of 1.0 and pressures of 20 bar and 47.4–51.2 bar. The measurements of laminar flame speed came from Zhao et al.[36] The gasoline surrogate has four components with a

https://doi.org/10.1021/acsomega.2c06515
ACS Omega 2023, 8, 3929−3944

Table 1. Composition in Cases 1−6

	syngas		gasoline surrogate				
case	H_2	CO	*n*-heptane	isooctane	toluene	diisobutene	volume proportion of syngas
1	0	0	20	25	45	10	0
2	5	5	18	22.5	40.5	9	10%
3	15	15	14	17.5	31.5	7	30%
4	25	25	10	12.5	22.5	5	50%
5	35	35	6	7.5	13.5	3	70%
6	45	45	2	2.5	4.5	1	90%

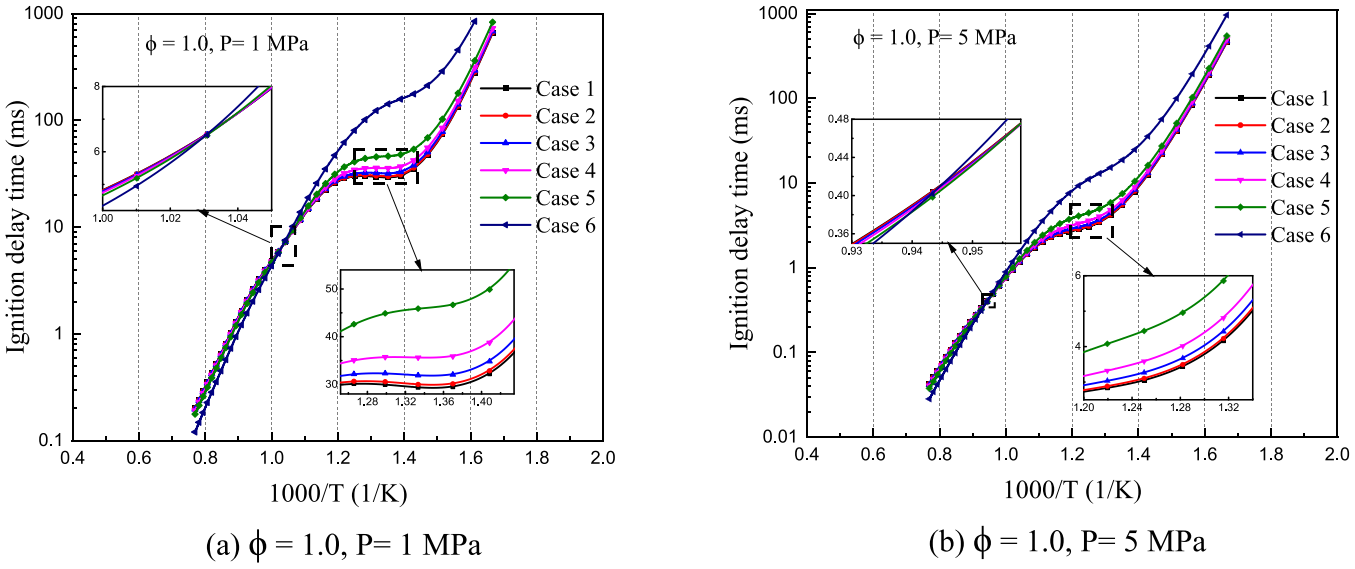

Figure 5. (a and b) Ignition delay times in Cases 1−6 under different pressures, ϕ = 1.0.

composition ratio of *n*-heptane (20%)/isooctane (25%)/toluene (45%)/diisobutylene (10%) by volume. As shown in Figure 2, the LLNL mechanism was consistent with the experimental data, which indicates that the mechanism has high accuracy.

A detailed chemical kinetic model of the syngas/gasoline blends was obtained by merging the Davis syngas mechanism into the LLNL mechanism, including 1389 species and 5942 reactions. Due to the lack of experimental data on syngas/gasoline blended fuel, the mechanism cannot be directly verified. Therefore, the existing experimental data on syngas, gasoline, and syngas/isooctane are used to verify the mechanism. Figure 3 compares the IDTs between the simulation and experimental data.[31,35] The results of the laminar flame speed are shown in Figure 4. Huang et al.[37] measured the laminar flame speed of syngas/isooctane blends in air at 0.1 MPa and 298 K; Zhao et al.[36] and Jerzembeck et al.[38] obtained the laminar flame speed of gasoline fuel in air at different temperatures and pressures.

The results shown in Figures 3 and 4 indicate that the mechanism of the syngas/gasoline mixture has high accuracy in predicting the IDTs and laminar flame speeds. Our mechanism can well demonstrate the combustion properties of syngas, gasoline, and their mixtures, and the predicted results are reliable. This mechanism will serve as the basis for the next section of the study.

3. RESULTS AND DISCUSSION

3.1. Effect of Syngas on the Ignition of Gasoline Surrogate/Air Mixtures. To investigate the effect of syngas fuel blending on the IDTs, six syngas/gasoline blends with different blending ratios were constructed. The volume ratio of gas components in syngas was fixed at H_2/CO = 1:1, and the liquid volume ratio of *n*-heptane/isooctane/toluene/diisobutylene in four-component gasoline surrogate fuels was 20/25/45/10, as shown in Table 1.

Figure 5 shows the various situations of the IDTs for Case 1−6 mixed fuel. The temperature ranged from 600 to 1300 K, and the pressures were 1 and 5 MPa. The obtained results show that the IDTs of the mixed fuel with a higher syngas ratio are not always higher than those with a lower syngas ratio. This phenomenon is reversed when the initial temperature exceeds a critical temperature of approximately 1000 K. Thus, the simulation results can be divided into a low-temperature region (T < 1000 K) and a high-temperature region (T > 1000 K).

In the low-temperature region, the IDTs of the mixture with a higher proportion of syngas are always longer than those with less syngas. In other words, the addition of syngas increases the IDTs of the fuel in the low-temperature reaction stage. Considering that the reaction rate of the system is mainly dominated by the oxidation reaction of gasoline C7−C8 macromolecules in the low-temperature region, the addition of syngas diluted the concentration of gasoline fuel, resulting in the slow oxidation rate of hydrocarbon molecules and a relative lag in the IDTs. On the other hand, in the high-temperature stage, the IDTs of the mixture with a high syngas ratio are slightly lower than those with a lower syngas ratio. It can be seen that with the initial temperature of the system rising to more than 1000 K, the effect of C0 small molecules in syngas on improving the reaction system activity is clear. At this time, the reaction rate of the system was more dependent on the reaction of small

https://doi.org/10.1021/acsomega.2c06515
ACS Omega 2023, 8, 3929−3944

Table 2. Composition in Cases 7−10

	syngas		gasoline surrogate				
case	H_2	CO	*n*-heptane	isooctane	toluene	diisobutene	H_2 proportion
7	0	50	10	12.5	22.5	5	0
8	15	35	10	12.5	22.5	5	30%
9	35	15	10	12.5	22.5	5	70%
10	50	0	10	12.5	22.5	5	100%

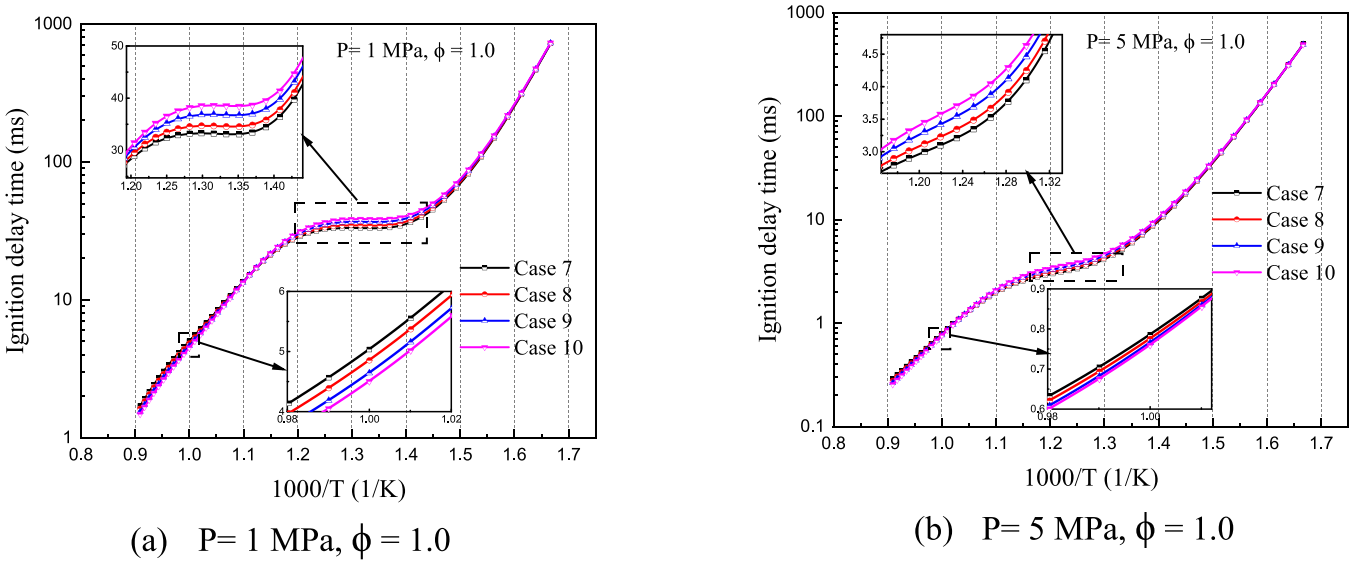

Figure 6. (a and b) Ignition delay times in Cases 7−10 under different pressures, ϕ = 1.0.

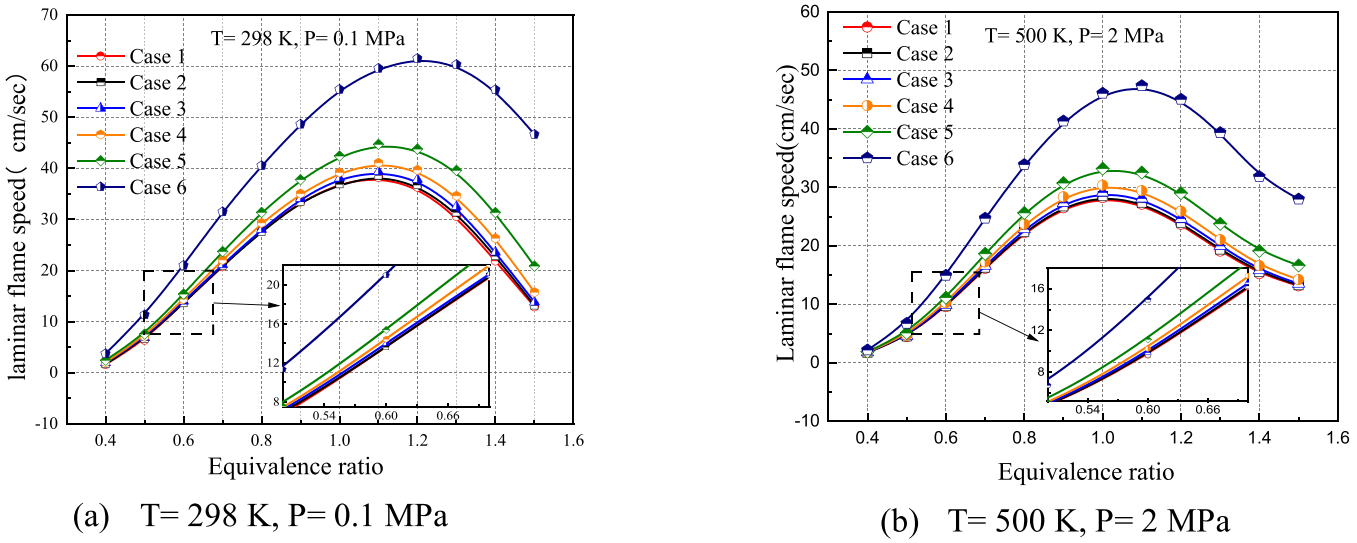

Figure 7. (a and b) Laminar flame speed in Cases 1−6 in the equivalence ratio range of 0.4−1.5 at different temperatures and pressures.

molecules and the ignition time was relatively earlier. In addition, the negative temperature coefficient (NTC) behavior of different fuel mixtures becomes less obvious when the initial pressure changes from 1 to 5 MPa, which also indicates that the addition of C0 molecules in syngas reduces the temperature range of the intermediate transition reaction zone.

The simulation results are further analyzed based on the GDI working mode of the gasoline engine. The knock combustion restricting the performance of the GDI engine is due to the low-temperature spontaneous combustion of the unburned mixture in the cylinder. Therefore, the delay on ignition caused by the incorporation of syngas is beneficial to the suppression of the spontaneous combustion of the unburned mixture. Figure 5 shows that mixed gasoline fuel with syngas can shorten the IDT in the high-temperature reaction region. Near the spark plug of the engine, the mixture is heated to more than 1000 K by a high-energy spark to produce a large number of active free radicals and ignite quickly. Therefore, the fuel blend near the spark plug can be seen as reacting directly to high temperatures and igniting quickly. The introduction of syngas can reduce the IDT of gasoline fuel near the spark plug, allowing the "fire core" to be produced more quickly. Therefore, in the cylinder combustion

https://doi.org/10.1021/acsomega.2c06515
ACS Omega 2023, 8, 3929−3944

Table 3. Composition in Cases 11−16

	syngas		gasoline surrogate				
case	H_2	CO	*n*-heptane	isooctane	toluene	diisobutene	H_2 proportion
11	0	90	2	2.5	4.5	1	0
12	18	72	2	2.5	4.5	1	20%
13	36	54	2	2.5	4.5	1	40%
14	54	36	2	2.5	4.5	1	60%
15	72	18	2	2.5	4.5	1	80%
16	90	0	2	2.5	4.5	1	100%

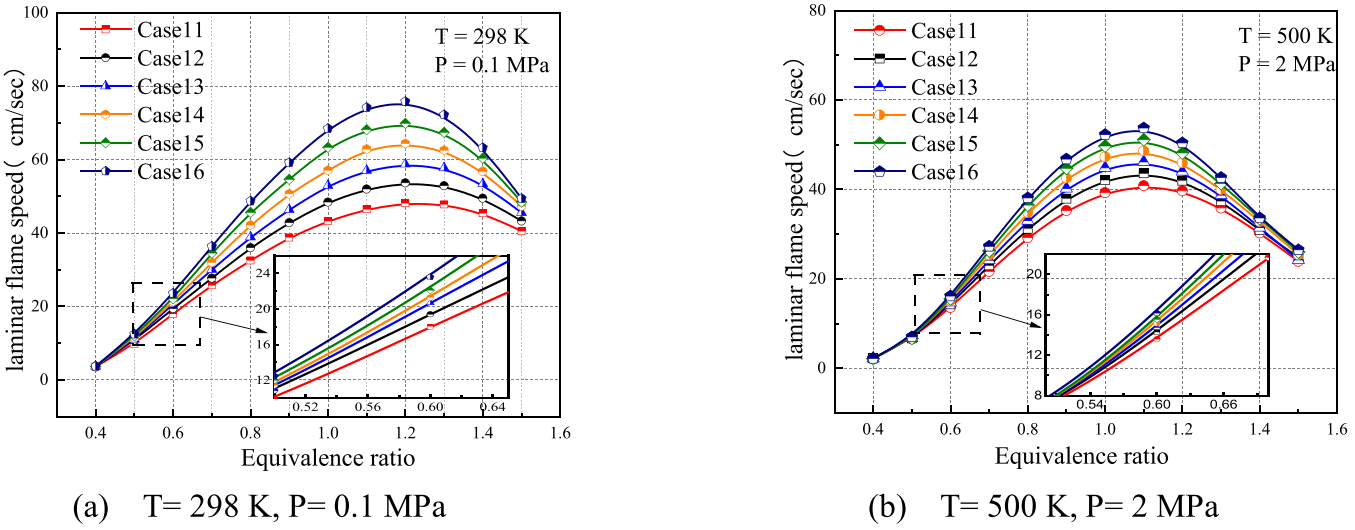

Figure 8. (a and b) Laminar flame speed in Cases 11−16 in the equivalence ratio range of 0.4−1.5 at different temperatures and pressures.

process of a GDI engine, the addition of syngas can inhibit the occurrence of knock combustion from two aspects: prolonging the spontaneous ignition time of the unburned mixture in the low-temperature oxidation zone and shortening the ignition lag period of the mixture in the high-temperature zone near the spark plug.

In addition, considering the different ways of obtaining syngas, the ratio of H_2 to CO in actual syngas fuel is uncertain. Therefore, to make the research results more widely representative, the influence of the H_2/CO ratio in syngas on the ignition delay of the mixture was studied. Four syngas/gasoline mixtures in Cases 7−10 were selected with a constant syngas blending ratio but gradually increasing the H_2 ratio in syngas, as shown in Table 2.

The effect on the IDTs caused by the ratio of H_2 to CO in syngas is shown in Figure 6. Its influence is similar to that caused by the blending ratio of syngas in gasoline. The entire temperature region can still be roughly divided into the low-temperature oxidation region and the high-temperature oxidation region. In the low-temperature region, the IDTs of the mixed fuel increase with the increase in the proportion of the H_2 component in the syngas, but the opposite is true in the high-temperature oxidation part. It can be seen that a larger H_2 fraction increases the oxidation reaction rate of the system in the high-temperature region, while in the low-temperature phase, it dilutes the macromolecular concentration of gasoline, thus inhibiting the oxidation reaction process. However, the influence of different H_2 ratios in syngas on IDT does not show significant differences. This indicates that in actual combustion, as long as the appropriate syngas/gasoline ratio is selected, the ignition and combustion requirements of the GDI engine can be met.

3.2. Effect of Syngas on the Laminar Flame Speed of Gasoline Surrogate/Air Mixtures. The laminar flame speed is one of the important parameters of fuel combustion. This section considers the effects of the mixing ratio of syngas and the internal ratio of syngas. The variation in the laminar flame speed with equivalence ratios under normal temperature and pressure (298 K and 0.1 MPa) and high temperature and high pressure (500 K and 2 MPa) was studied, as shown in Figure 7.

Under different inlet conditions, the increase in the proportion of syngas accelerates the laminar flame speeds. The reason for this phenomenon is that the H_2 component in syngas can enhance the reactivity of the reaction system, increase the flame propagation speed, and play a role in stabilizing combustion. At the same time, it shortens the time of the flame front passing to the end mixture. This trend has a certain effect on inhibiting the detonation combustion of gasoline engines. In addition, the equivalent ratio corresponding to the peak point of the flame speed is also larger, indicating that the addition of syngas can make the blended fuel reach the peak flame propagation speed at higher concentrations.

In addition, it can be found that the equivalence ratio corresponding to the maximum laminar flame speed in Figure 7a is larger than that in Figure 7b. Taking Cases 1−5 as examples, the corresponding equivalence ratio is 1.1 in Figure 7a, which is reduced to 1.0 in Figure 7b, indicating that more air is required for the fastest propagation of syngas/gasoline blends at higher temperatures and pressures. The large proportion of syngas leads to a large difference between Case 6 and the other data, indicating that syngas greatly affects the laminar flame speed.

https://doi.org/10.1021/acsomega.2c06515
ACS Omega 2023, 8, 3929−3944

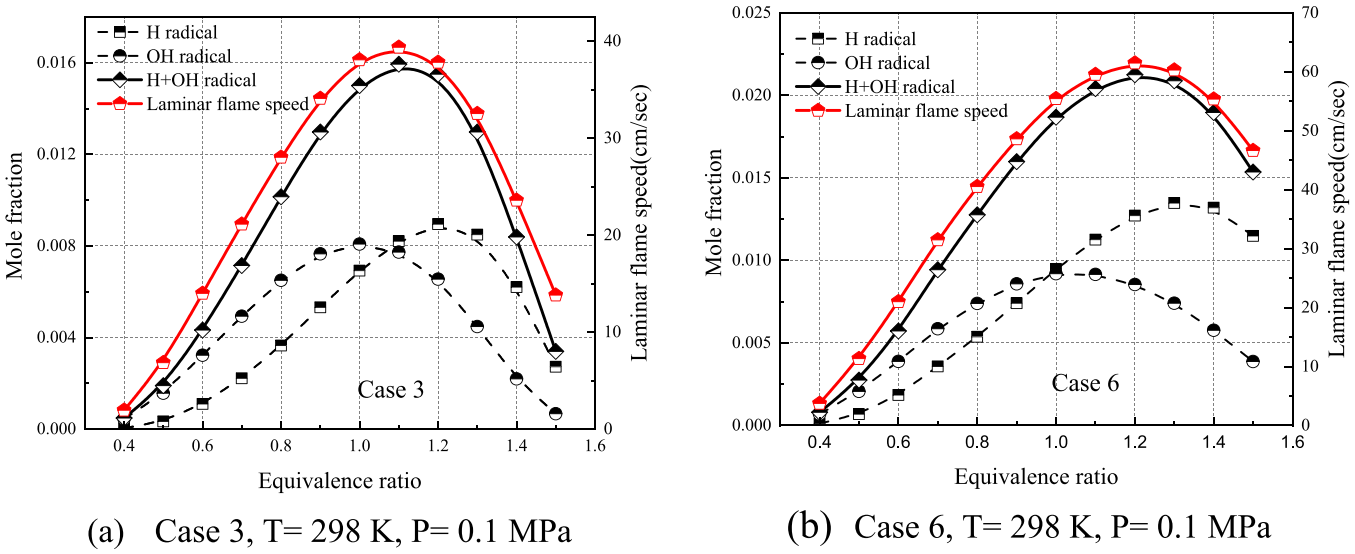

Figure 9. (a and b) H, OH, and H + OH concentrations and laminar flame speeds in Cases 3 and 6, T = 298 K, P = 0.1 MPa, and ϕ = 0.4−1.5.

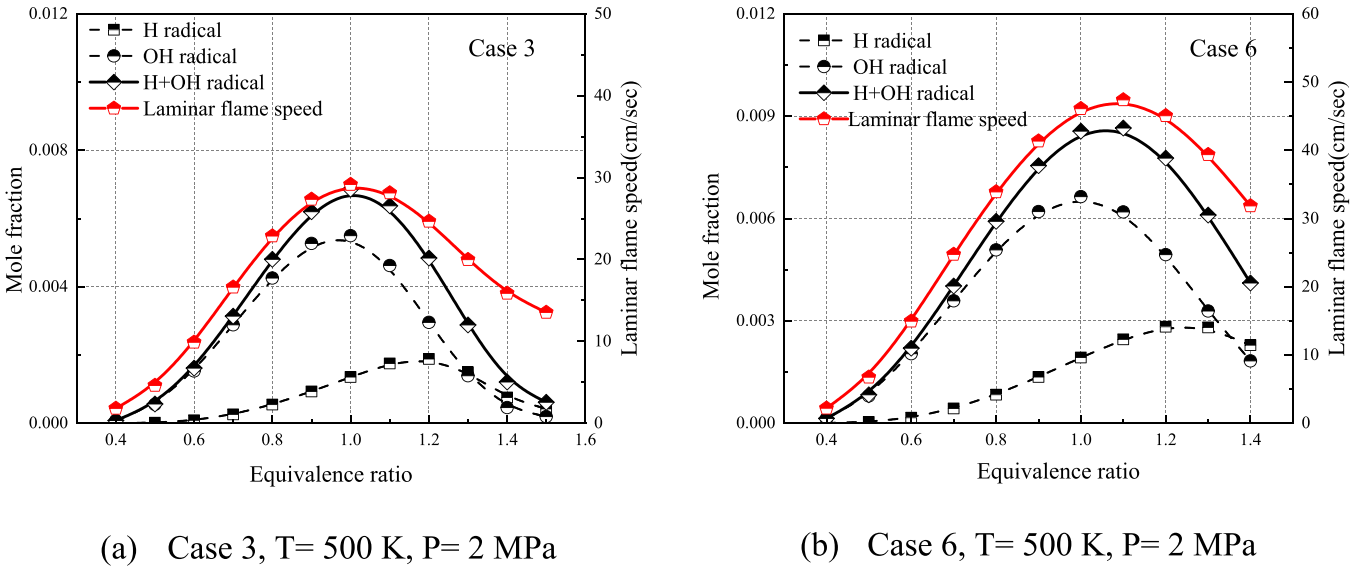

Figure 10. (a and b) H, OH, and H + OH concentrations and laminar flame speeds in Cases 3 and 6, T = 500 K, P = 2 MPa, and ϕ = 0.4−1.5.

The influence of the H_2/CO ratio on the laminar flame speeds was also considered. The internal component ratio of gasoline substitutes is the same as that in the previous proportion. To make the effect of the H_2/CO ratio in syngas on the laminar flame speeds of syngas/gasoline blends more obvious, the mixing ratio of syngas is fixed at 90% by volume fraction and the H_2/CO ratio changes from 0:90 to 90:0, as shown in Table 3. The laminar flame speeds in Cases 11−16 with equivalence ratios under different inlet conditions are shown in Figure 8.

The obtained results show that the laminar flame speeds of the mixed fuel with different H_2/CO ratios in syngas vary with the equivalence ratio. When the equivalence ratio is 0.4, the laminar flame speeds of all cases are very small and very close. When the equivalence ratio increases, the laminar flame speed of the mixture fuel with a higher volume fraction of H_2 in the syngas increases faster, as shown in Figure 8, and the variation curve of all cases gradually becomes steeper. This indicates that more H_2 components in the syngas help to accelerate the flame propagation speed and improve the combustion stability in the lean combustion region.

By comparing Figure 8a,b, it is determined that the laminar flame speeds in Cases 11−16 decreased at higher temperature and pressure levels and the equivalence ratio corresponding to the peak flame velocity changed from 1.2 at room temperature and atmospheric pressure to 1.1, indicating that the amount of air required for the combustion of the syngas/gasoline mixture to reach the fastest flame propagation velocity at higher temperature and pressure levels decreased.

3.3. Concentration Analysis of Active Free Radicals.

The concentrations of free radicals such as H and OH in the flame front were shown to be closely connected to the laminar flame propagation speed of fuel in reference.[39] To learn more about the combustion properties of the mixture, this work investigates the laminar flame speeds of syngas/gasoline mixtures with the concentrations of H and OH radicals in the one-dimensional laminar flame reaction system.

Under different conditions, the mole fraction of H, OH, and H + OH radicals and laminar flame speeds in Cases 3 and 6 are shown in Figures 9 and 10. The trends of all parameters increase first and subsequently decrease as ϕ increases. The curve shape

https://doi.org/10.1021/acsomega.2c06515
ACS Omega 2023, 8, 3929−3944

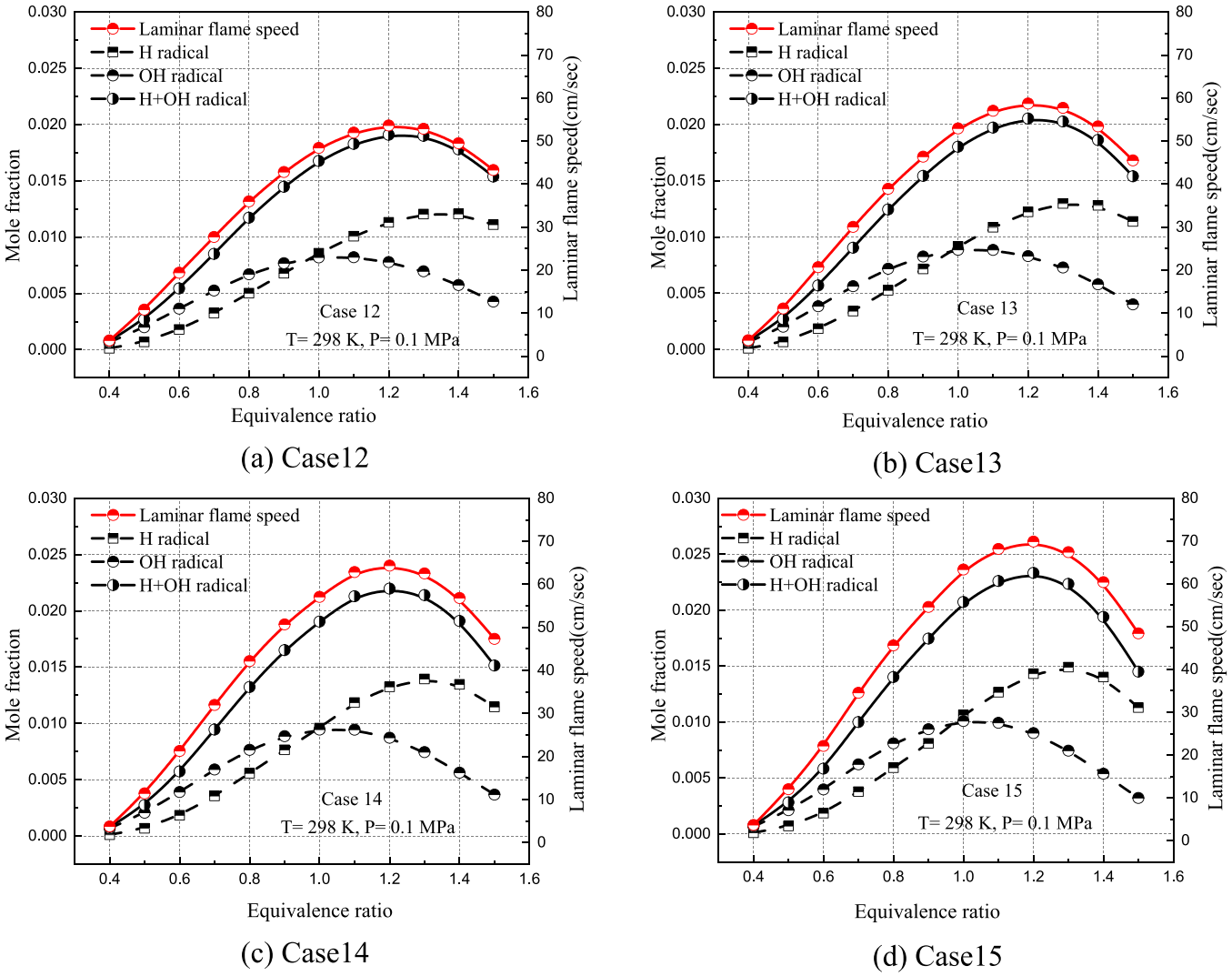

Figure 11. (a–d) H, OH, and H + OH concentrations and laminar flame speeds in Cases 12–15, T = 298 K, and P = 0.1 MPa.

of the laminar flame speed and the related ϕ of the peak heat release rate are largely compatible with the total H + OH concentration. Both the H and OH radical concentrations affect the sum of the H + OH radical concentrations.

In Figure 9, the OH mole fraction of Case 3 peaked at approximately ϕ = 1.0, while the H peaked at approximately ϕ = 1.2, with the H radical peak concentration only slightly higher than the OH radical peak concentration. At ϕ = 1.1, the sum of the H + OH concentrations reached its maximum, which was the same as the maximum laminar flame speed. The concentration of OH radicals reaches its greatest value at approximately ϕ = 1.0 in Case 6, whereas the equivalence ratio increases to 1.3 when the concentration of H radicals reaches its maximum value. The addition of more syngas, particularly H_2, increases the peak concentration of H radicals much more than the peak concentration of OH radicals, resulting in the H + OH concentration in Case 6 reaching its maximum value at a larger ϕ (approximately 1.2). The peak laminar flame speed significantly increases compared to Case 3, which is the deep-seated reason for the delay of the peak laminar flame speed to the equivalence ratio in Cases 6 to 1.2.

Figure 10 shows that the peak concentration of H radicals is only 1/3–1/2 that of OH radicals, although H radicals and OH radicals both reach their maximum values at equivalence ratios of 1.2 and 1.0, respectively, which differs from the data in Figure 9a. As previously stated, the H and OH mole fractions affect the variation curve of the laminar flame speed and H + OH concentration. Therefore, it can be concluded that at higher temperatures and pressures, the variation of syngas/gasoline laminar flame speeds with equivalence ratios will be more dependent on the change of OH radical concentration, which also leads to the change of the equivalence ratio corresponding to the peak point of laminar flame speed at high temperatures and high pressures.

The effect of the H_2 ratio in syngas on active radical concentrations and laminar flame speeds was studied. The variations in the H, OH, and H + OH radical concentrations and laminar flame velocity of the syngas/gasoline mixture in Cases 12–15 were analyzed under different conditions, as shown in Figures 11 and 12. The equivalence ratio increased from 0.4 to 1.5. The H + OH concentration curve was found to be essentially compatible with the laminar flame velocity curve and achieved its maximum value at an equivalent ratio of approximately 1.2. The matching peak value grows in proportion to the H_2 fraction in the syngas.

When the equivalence ratio increases from 0.4 to 1.0, the concentration of the OH radical is always greater than the concentration of the H radical and the growth rate of the OH

https://doi.org/10.1021/acsomega.2c06515
ACS Omega 2023, 8, 3929–3944

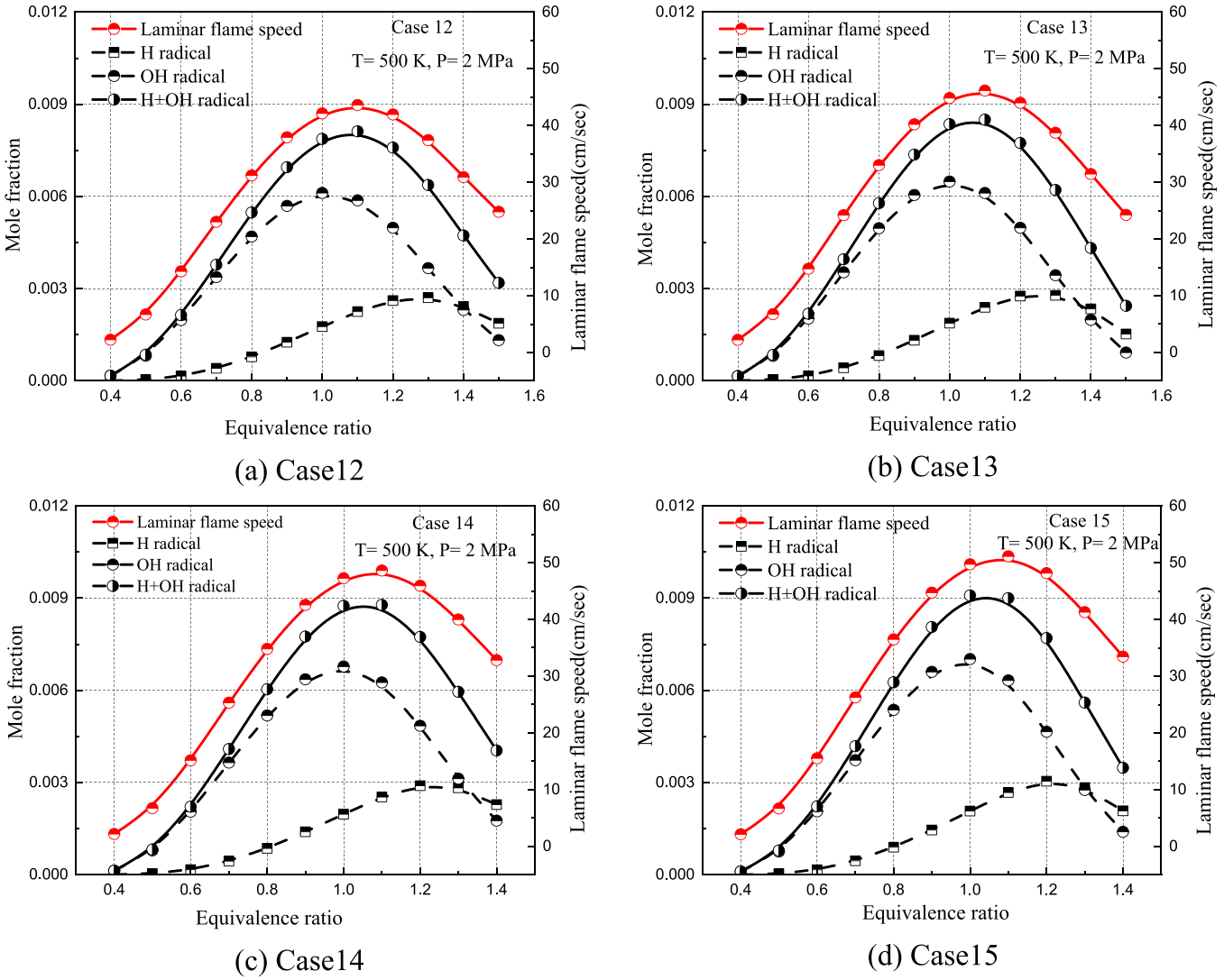

Figure 12. (a–d) H, OH, and H + OH concentrations and laminar flame speeds in Cases 12–15, T = 500 K, and P = 2 MPa.

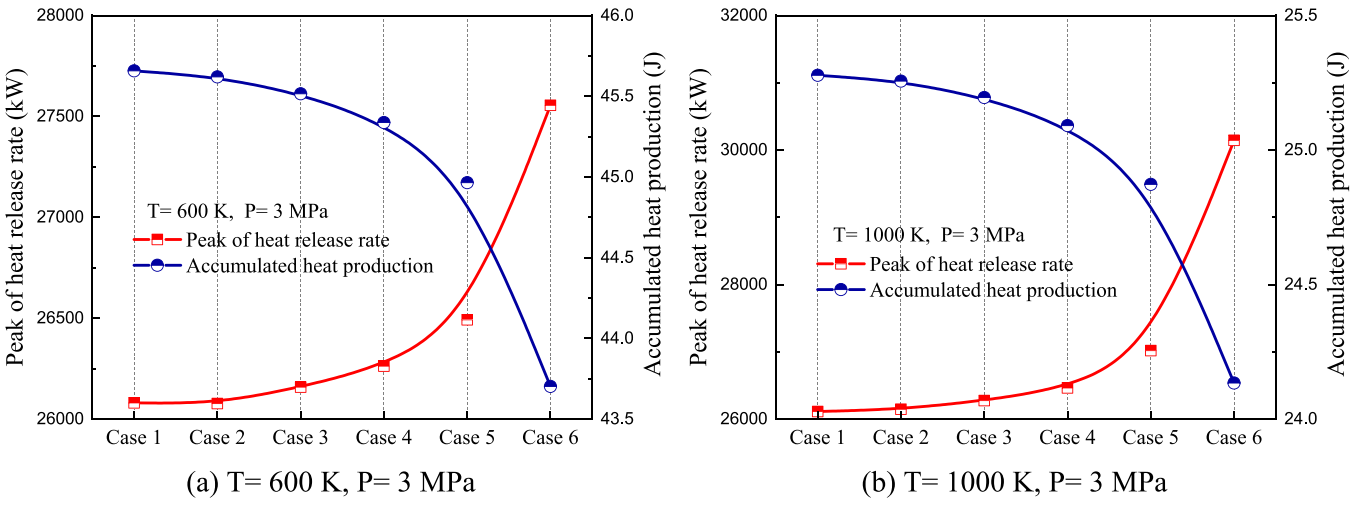

Figure 13. (a and b) Peak heat release rate and accumulated heat production in Cases 1–6 at ϕ = 1.0.

concentration slows down, while the growth rate of the H concentration accelerates. When the equivalence ratio is greater than 1.0, the concentration of H free radicals exceeds that of OH free radicals and the latter begins to decline from this point, while the former begins to increase toward an equivalence ratio of 1.3. Furthermore, it was discovered that when H_2 was added to syngas, the peak concentration of H free radicals was substantially higher than that of OH free radicals.

https://doi.org/10.1021/acsomega.2c06515
ACS Omega 2023, 8, 3929−3944

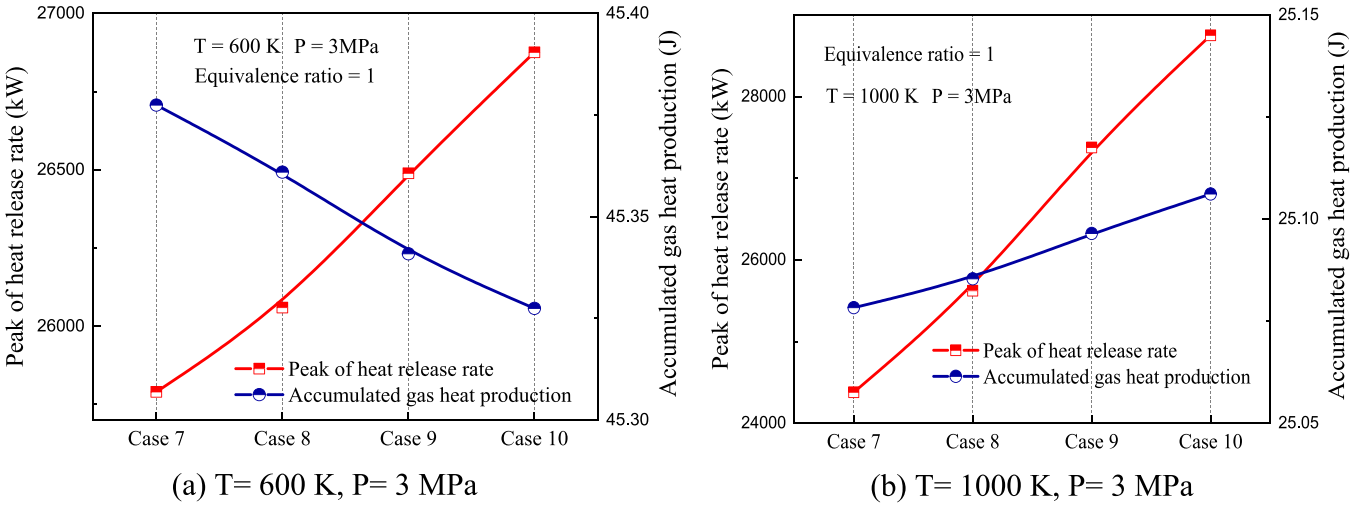

Figure 14. (a and b) Peak heat release rate and accumulated heat production in Cases 7−10 at ϕ = 1.0 and P = 3 MPa.

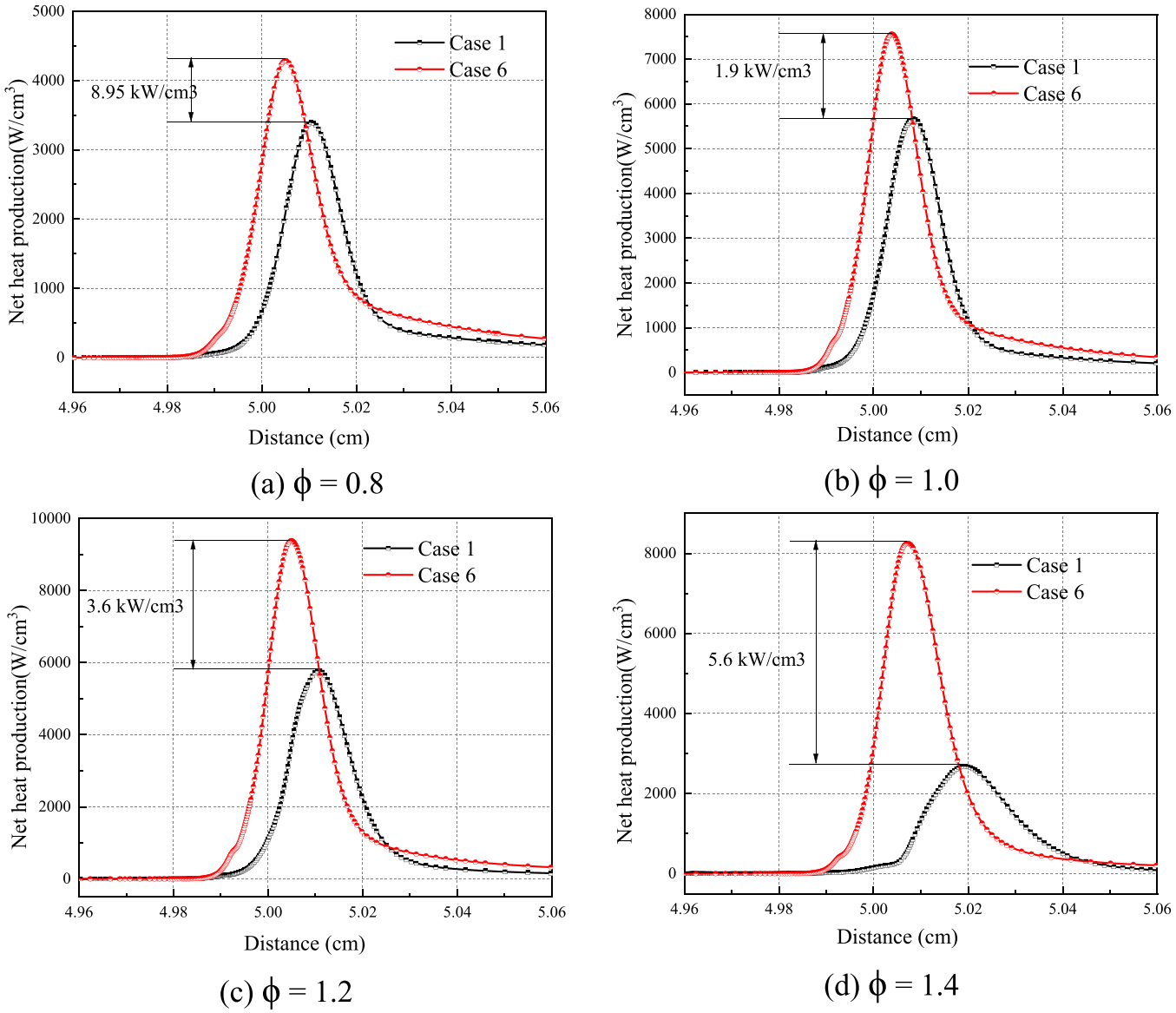

Figure 15. (a−d) Net heat production in Cases 1 and 6, T = 298 K, and P = 0.1 MPa.

https://doi.org/10.1021/acsomega.2c06515
ACS Omega 2023, 8, 3929−3944

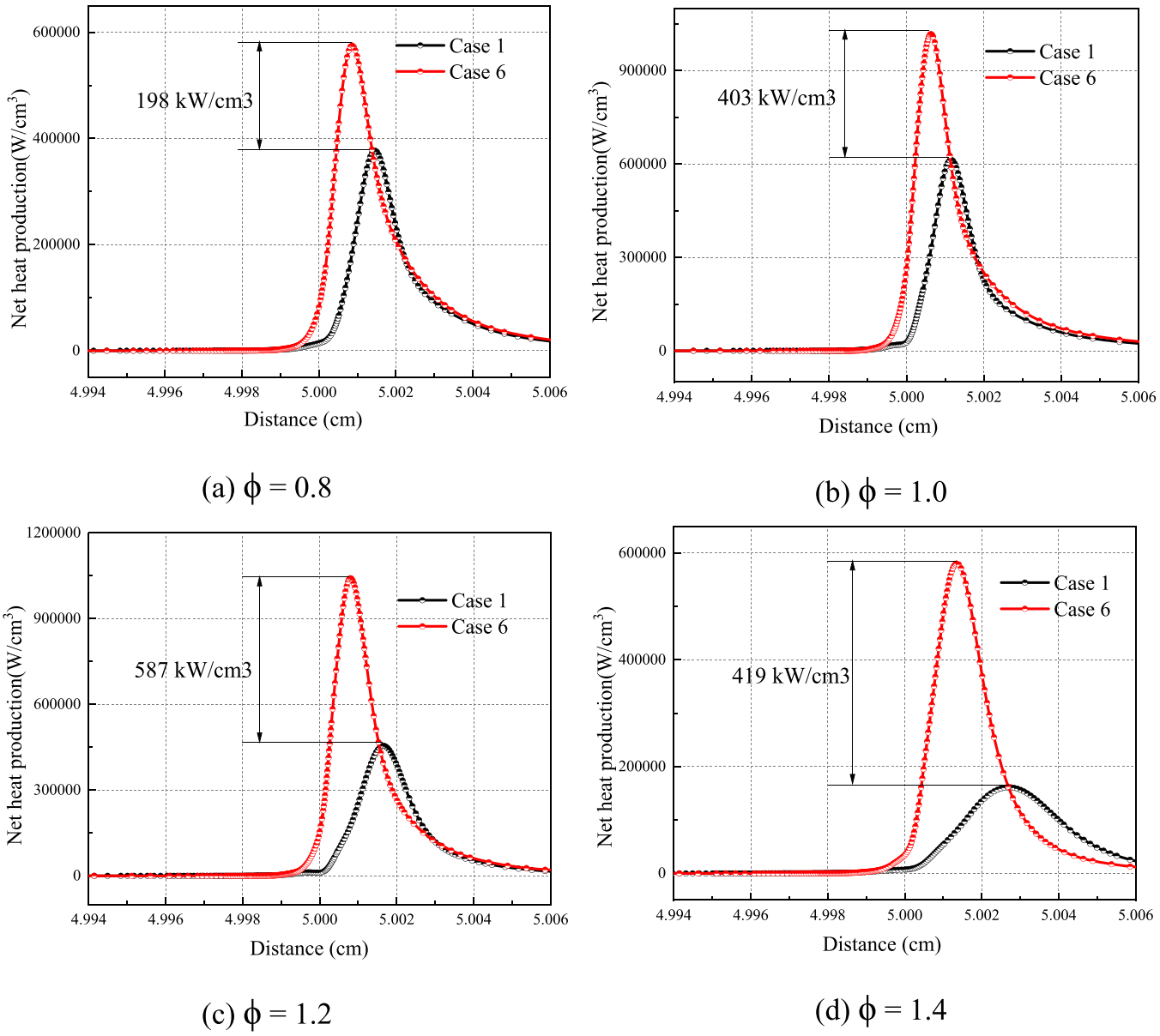

Figure 16. (a–d) Net heat production in Cases 1 and 6, T = 500 K, and P = 2 MPa.

Although the concentration peaks of the H and OH free radicals are still near equivalence ratios of 1.2 and 1.0, as shown in Figure 12, their molar concentrations are substantially different. The peak concentration of H radicals was higher than that of OH radicals at 298 K/0.1 MPa but only 1/3–1/2 of the peak concentration of OH radicals at 500 K/2 MPa. Similar to earlier findings, the fluctuation of syngas/gasoline laminar flame speeds with equivalency ratios is more dependent on the variation of OH radical concentration in the flame front at higher temperatures and pressures.

3.4. Effect of Syngas on the Heat Release of Gasoline Surrogate/Air Mixtures. Although the incorporation of syngas can reduce the tendency of engine knock combustion, due to its low calorific value, a higher mixing ratio of syngas is not better. The effect of syngas addition on heat release was further analyzed.

Figure 13 shows the increasing proportion of syngas in the mixed fuel in Cases 1–6. The obtained results indicate that although the addition of syngas increases the peak of the heat release rate of the blended fuel, the accumulated heat production continuously decreases and the time of heat release of the mixed fuel with a higher syngas ratio is shorter for the combustion process belonging to the heat release process. The syngas addition will increase the reaction rate in the high-temperature region, leading to a more intense exothermic process. However, limited to the low calorific value of syngas, it does not increase the levels of total heat quantity, which is one of the main reasons that limits the amount of added syngas. In addition, the peak of the heat release rate at the high temperature of the 1000 K fuel oxidation zone is always higher than that at 600 K, while the trend of accumulated heat production is the opposite. This shows that the exothermic reaction in the high-temperature stage is more intense, but the exothermic reaction that begins in the low-temperature reaction stage of the combustion process can release more heat.

The influence of the H_2/CO ratio in syngas on the exothermic process is shown in Figure 14. In Figure 14a, with the increasing proportion of H_2, the peak heat production rate gradually

https://doi.org/10.1021/acsomega.2c06515
ACS Omega 2023, 8, 3929–3944

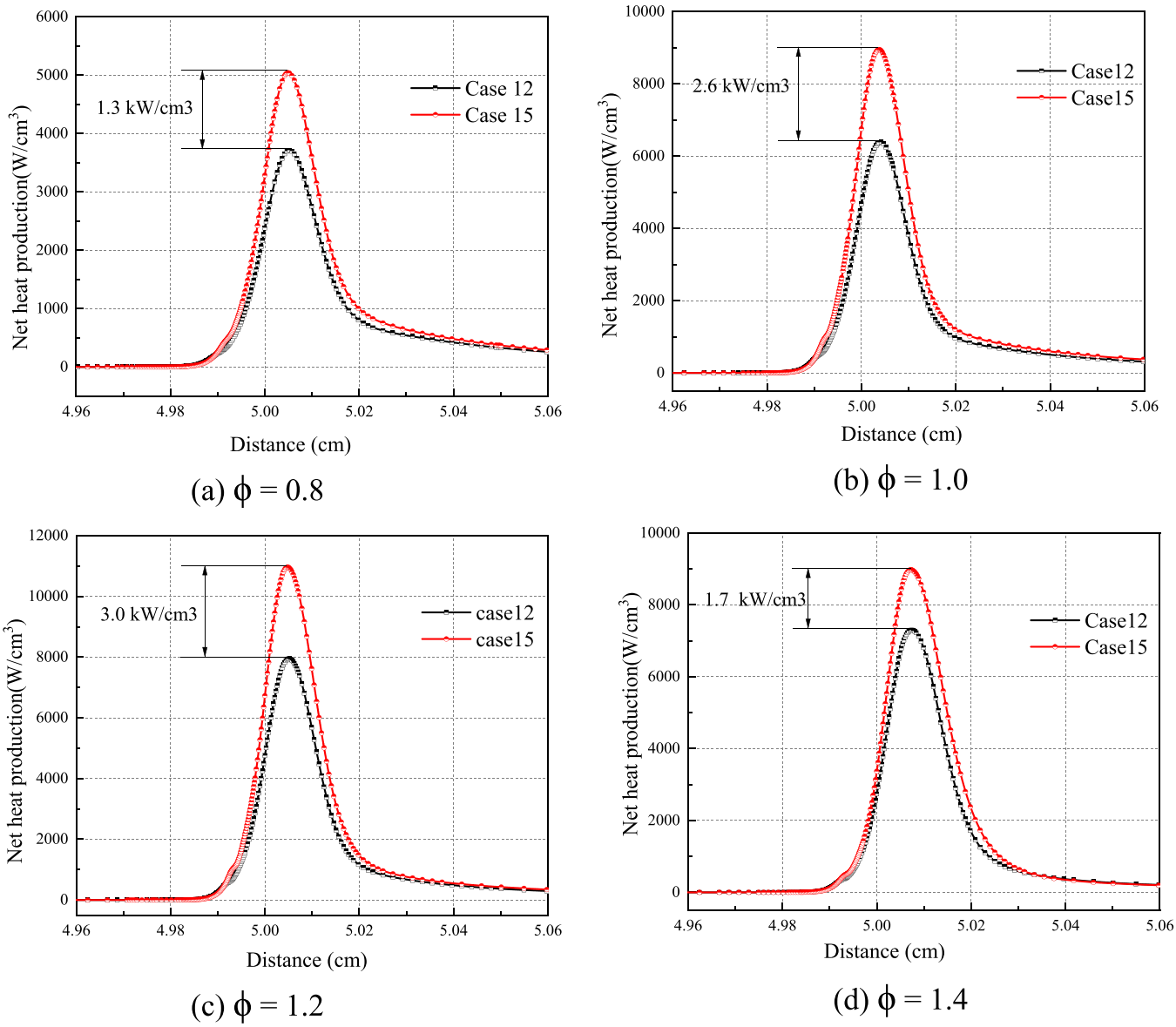

Figure 17. (a–d) Heat release in Cases 12 and 15, T = 298 K, and P = 0.1 MPa.

increases and the accumulated heat production gradually decreases. The difference between the peak heat release rates in Cases 7 and 10 is approximately 1000 kW. However, in Figure 14b, the two parameters increase to varying degrees with increasing H_2 ratios and the peak heat release rate in Cases 7–10 varies by approximately 4000 kW. Although H_2 contributes to the complete combustion of fuel, the increase in the H_2 ratio has little effect on the accumulated heat production during combustion (approximately 0.05 J at a low temperature and 0.025 J at a high temperature). Therefore, a higher initial reaction temperature and higher H_2 ratio in syngas can help shorten the exothermic time and make the combustion and exothermic processes more intense.

In Figure 14a,b, the trend of accumulated heat production is different with the increase of hydrogen. Since the calorific value of hydrogen is lower than that of CO, the increase of H2 and the decrease of CO lead to a decrease in the calorific value of the fuel mixture and, therefore, a decrease in the heat released from the fuel. At the same time, the increase in hydrogen promotes complete combustion and reduces HC and CO emissions, when more heat is released. Both of these effects have an impact on the cumulative heat production. At 600 K, the heat loss due to the low calorific value is greater than the heat added by complete combustion, so the accumulated heat is reduced. At 1000 K, the system is more active and reactive, which also leads to inadequate reactions and higher HC and CO emissions. The heat added by complete combustion is greater than the losses due to the low calorific value. Thus, at 1000 K, the accumulated heat increases with the increase of hydrogen. This is consistent with the emission performance observed in Figure 20 in Section 3.5.

Next, starting from the heat release curve of the one-dimensional flame propagation process of the mixed fuel, the thickness of the laminar flame is quantitatively characterized by the one-dimensional heat release interval size of the laminar flame. Case 1 of the pure gasoline condition and Case 6 of the syngas mixing condition are taken to indirectly analyze the heat release process and structural characteristics of the laminar flame in one-dimensional space, respectively. The conditions of the study were 298 K at 0.1 MPa and 500 K at 2 MPa, and the

https://doi.org/10.1021/acsomega.2c06515
ACS Omega 2023, 8, 3929−3944

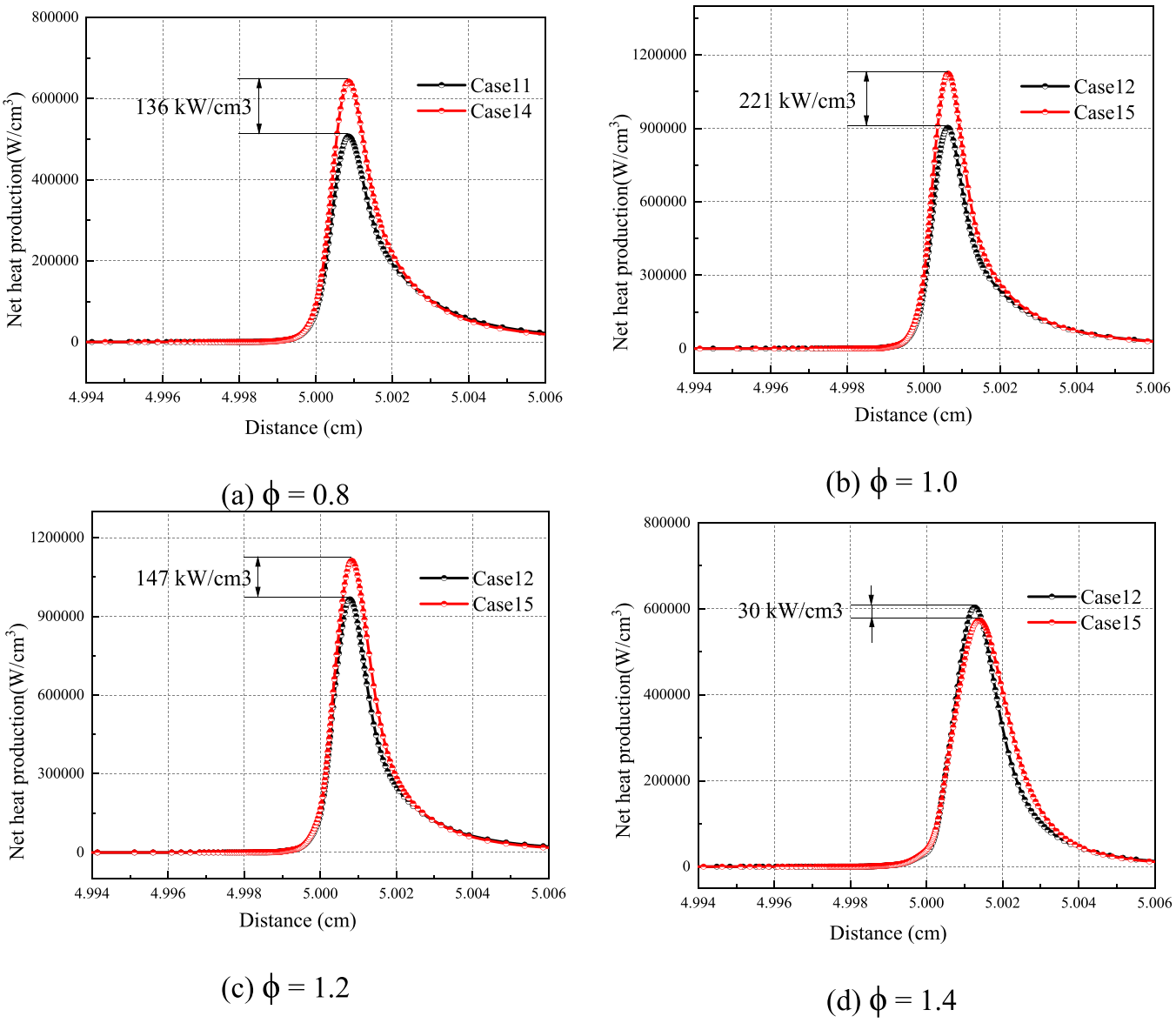

Figure 18. (a–d) Heat release in Cases 12 and 15, T = 500 K, and P = 2 MPa.

equivalence ratio increased from 0.8 to 1.4. The obtained results are shown in Figures 15 and 16.

The obtained results show that the net heat production in Case 6 is higher than that in Case 1 under the same conditions. The initial position and end position of heat release are earlier than those in Case 1 (the flame front is also more forward), and the process of heat release is more intense. In addition, with the increase in equivalence ratio, the peak heat release of the two mixtures first increases and then decreases. The equivalence ratio corresponding to the maximum net heat production is in the range of 1.0–1.2, which is consistent with the trend of laminar flame speed with the equivalence ratio. Comparing Figures 15 and 16, it is found that the laminar flame morphology was quite different. In terms of the thickness of the heat release zone, the size of the heat release zone in Figure 16 is approximately 1/10 of that in Figure 15. For example, when the equivalence ratio is 1, the thickness of the heat release zone in Case 6 is approximately 0.02 cm in Figure 15, while it is only 0.002 cm in Figure 16. However, in the difference in net heat production, the latter (587 kW/cm^3) is hundreds of times greater than that of the former (3.6 kW/cm^3). It can be speculated that at higher temperature and pressure levels, the laminar flame of syngas/gasoline blends releases more heat in a thinner one-dimensional flame front.

Considering the influence of the H_2/CO ratio in syngas on the heat release and flame front structure in the combustion process of hybrid fuel, Cases 12 and 15 were selected for comparative analysis of the one-dimensional heat release curves. As shown in Figures 17 and 18, the combustion air equivalence ratio varies from 0.8 to 1.4 and the temperature and pressure are 298 K and 0.1 MPa, and 500 K and 2 MPa.

The obtained results shown in Figure 17 show that under the initial conditions of 298 K and 0.1 MPa, with ϕ increasing from 0.8 to 1.4, the net heat production of both cases first increases and then decreases and the difference between Cases 12 and 15 is also the same. The maximum value of the difference was 3.0 kW/cm^3 obtained at ϕ = 1.2. In addition, Case 15, with a higher H_2 ratio, always had a higher exothermic peak than Case 12.

The difference in heat release between Cases 12 and 15 under 500 K/2 MPa conditions shown in Figure 18 is far less obvious

https://doi.org/10.1021/acsomega.2c06515
ACS Omega 2023, 8, 3929−3944

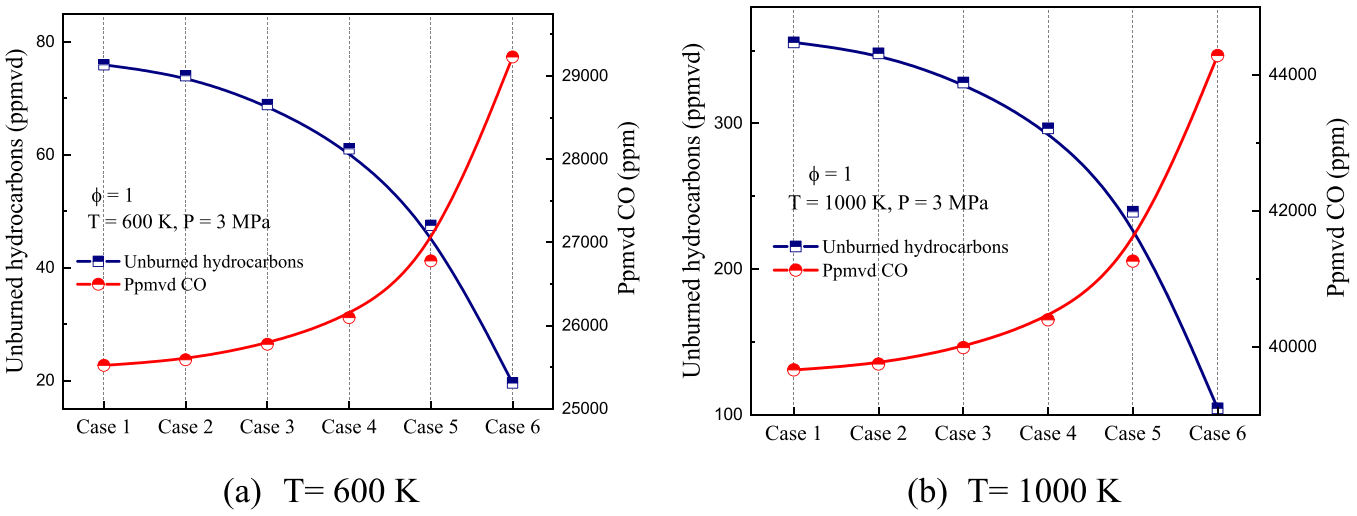

Figure 19. (a and b) Emissions of HC and CO in Cases 1−6 with different temperatures at pressures of 3 MPa and ϕ = 1.0.

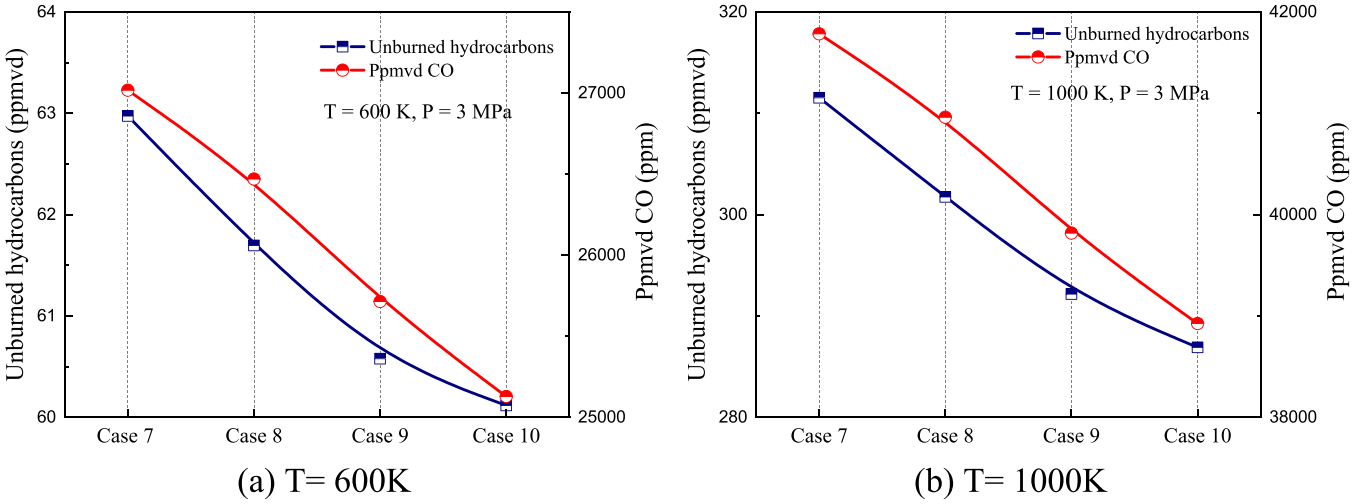

Figure 20. (a and b) Emissions of HC and CO in Cases 7−10 with different temperatures at pressures of 3 MPa and ϕ = 1.0.

than that in Figure 17. Even when ϕ = 1.4, the net heat production in Case 12 exceeds that in Case 15 by 30 kW/cm^3. In terms of the thickness of the one-dimensional heat release zone, the size of the flame heat release zone at 500 K/2 MPa is approximately 1/10 of that under normal temperature and pressure. This result is consistent with the abovementioned conclusion that at higher temperature and pressure levels, the laminar flame of syngas/gasoline blends emits more heat at a smaller scale.

Furthermore, the starting and ending positions of the heat release in Cases 12 and 15 are essentially constant under the two working conditions, indicating that the H_2 ratio in the syngas has no effect on the thickness of the laminar flame heat release zone (as shown in Figures 17 and 18). This conclusion differs dramatically from the findings of earlier studies on the effect of the syngas/gasoline ratio. As a result, it is possible that the thickness of the one-dimensional laminar flame exothermic zone of a syngas/gasoline combination is largely determined by the premixed syngas/gasoline ratio and is practically unaffected by the ratio of H_2/CO in syngas.

3.5. Effect of Syngas on HC and CO Emissions of Gasoline Surrogate/Air Mixtures. As mentioned above, adding syngas to gasoline fuel can suppress the occurrence of knock combustion in gasoline engines, but the mixing ratio of syngas is limited by related factors. One limitation is the heat release of combustion mentioned above. On the other hand, the restriction comes from emissions. In this section, the emissions of HC and CO during the combustion of syngas/gasoline blends are considered.

Figures 19 and 20 show the effect of the syngas blending ratio and H_2 ratio in syngas on the emission, respectively. The pressure is 3 MPa, the equivalence ratio is 1.0, and the initial reaction temperatures are 600 and 1000 K, respectively.

The obtained results show that with the increase in syngas proportion in the blended fuel, the emission concentration of HC decreases, while the emission concentration of CO gradually increases. Both HC and CO emissions at 600 K are less than those at 1000 K, indicating that starting from the low-temperature oxidation stage is conducive to reducing the emissions of HC and CO. Although the high temperatures increase activity and the reaction rate, it may also cause more severe incomplete combustion. On the other hand, with the increase in H_2 in syngas, the emissions of HC and CO linearly decrease, whether the reactions start at low or high temperature, which indicates that H_2 in syngas contributes to the full

https://doi.org/10.1021/acsomega.2c06515
ACS Omega 2023, 8, 3929−3944

combustion of syngas/gasoline blends and reduces the emissions of related pollutants.

4. CONCLUSIONS

A detailed chemical kinetic mechanism for syngas/gasoline blends has been constructed, containing 1389 species and 5942 reactions. In the mechanism validation, the predicted results are in good agreement with the experimental data. The effect of syngas addition on the ignition and combustion characteristics of gasoline fuels was investigated using this mechanism. Important observations are as follows:

(1) With the addition of syngas, IDT in the high-temperature region decreases, but in the low-temperature region, IDT increases. Increasing the H_2/CO ratio has little effect on the IDT when the syngas blending ratio is 50%. The addition of syngas can inhibit the occurrence of knock combustion from two aspects: prolonging the spontaneous ignition time of the unburned mixture in the low-temperature oxidation zone and shortening the ignition lag period of the mixture in the high-temperature zone near the spark plug.

(2) The addition of syngas, especially the increase in the proportion of H_2, promotes the activity of the reaction system and increases the laminar flame speed of the fuel. It is also good for inhibiting knock combustion and improving combustion stability. Furthermore, as the temperature and pressure increase, the amount of air required to reach the maximum laminar flame speeds decreases.

(3) The OH and H radical concentrations affect the variation trend of laminar flame speeds of syngas/gasoline with equivalence ratios. The addition of syngas, particularly the increase in the H_2 component, boosted the concentration of H free radicals. The equivalent ratio corresponding to the peak value of the H + OH concentration was delayed under normal temperature and pressure conditions, causing the laminar flame speed peak to be delayed. The fluctuation in flame speed with the equivalency ratio is more dependent on the concentration of OH radicals in the flame front at higher temperatures and pressures.

(4) The peak of the heat release rate in the zero-dimensional combustion process accelerates as the fraction of syngas in the mixed fuel increases, but the accumulated heat production decreases. The peak of the heat release rate increases as the fraction of H_2 in syngas increases, and the change in accumulated heat production is dependent on the temperature level. At high temperatures, the increase in heat due to complete combustion is greater than the heat loss due to the calorific value reduction and the overall accumulated heat production increases. The flame front was found to be closer to the fuel inlet when the quantity of syngas in the mixed fuel and the H_2/CO ratio in the syngas were increased, and the exothermic process was more intense. The heat release thickness of a one-dimensional laminar flame is largely determined by the premixed syngas/gasoline ratio and is practically unaffected by the H_2/CO ratio in syngas.

(5) The addition of syngas, especially the increase in the proportion of H_2, favors the promotion of complete combustion and the reduction of HC emissions but also brings an additional increase in CO. Combustion at lower temperatures has lower CO and HC emissions.

AUTHOR INFORMATION

Corresponding Author

Zhaolei Zheng − *Key Laboratory of Low-Grade Energy Utilization Technologies and Systems, Ministry of Education, Chongqing University, Chongqing 400044, China;* orcid.org/0000-0003-2905-0549; Email: zhengzhaolei@cqu.edu.cn

Authors

Qin Chen − *Key Laboratory of Low-Grade Energy Utilization Technologies and Systems, Ministry of Education, Chongqing University, Chongqing 400044, China*

Ziji Zhu − *Propulsion Control and Integration Application Department, SAIC Motor Passenger Vehicle Co., Shanghai 201804, China*

Complete contact information is available at: https://pubs.acs.org/10.1021/acsomega.2c06515

Author Contributions

Q.C., Z.Z., and Z.Z. conceived and designed the study. Z.Z. and Q.C. performed the experiments. Q.C. wrote the paper. Q.C., Z.Z., and Z.Z. reviewed and edited the manuscript. All authors read and approved the manuscript.

Notes

The authors declare no competing financial interest.

ACKNOWLEDGMENTS

This work was supported by the Special Key Project of Chongqing Technology Innovation and Application Development (Grant nos. cstc2020jscx-dxwtBX0024 and cstc2021jscx-dxwtBX 0024).

REFERENCES

(1) Xinquan, L.; Xiaofeng, Y. Challenges of China's Energy Strategy and the Reference from International Experience. *Globalization* **2022**, 107−115.

(2) Qian, Y., *China has nearly 400 million motor vehicles in 2021*; China Quality Daily, 2022, 006.

(3) Chunling, W.; Yingquan, C.; Liang, Z.; Zhang, G. Technical path for light duty gasolin vehicle to meet China VI emission regualtion. *Automobile Appl. Technol.* **2017**, 103−104.

(4) Park, H.; Lee, J.; Jamsran, N.; Oh, S.; Kim, C.; Lee, Y.; Kang, K. Comparative assessment of stoichiometric and lean combustion modes in boosted spark-ignition engine fueled with syngas. *Energy Convers. Manage.* **2021**, *239*, No. 114224.

(5) Jamsran, N.; Park, H.; Lee, J.; Oh, S.; Kim, C.; Lee, Y.; Kang, K. Influence of syngas composition on combustion and emissions in a homogeneous charge compression ignition engine. *Fuel* **2021**, *306*, No. 121774.

(6) Kravos, A.; Seljak, T.; Rodman Oprešnik, S.; Katrašnik, T. Operational stability of a spark ignition engine fuelled by low H2 content synthesis gas: Thermodynamic analysis of combustion and pollutants formation. *Fuel* **2020**, *261*, No. 116457.

(7) Mustafi, N. N.; Miraglia, Y. C.; Raine, R. R.; Bansal, P. K.; Elder, S. T. Spark-ignition engine performance with 'Powergas' fuel (mixture of CO/H2): A comparison with gasoline and natural gas. *Fuel* **2006**, *85*, 1605−1612.

(8) Paykani, A.; Chehrmonavari, H.; Tsolakis, A.; Alger, T.; Northrop, W. F.; Reitz, R. D. Synthesis gas as a fuel for internal combustion engines in transportation. *Prog. Energy Combust. Sci.* **2022**, *90*, No. 100995.

(9) Hagos, F. Y.; Aziz, A. R. A.; Sulaiman, S. A. Trends of Syngas as a Fuel in Internal Combustion Engines. *Adv. Mech. Eng.* **2014**, *6*, No. 401587.
(10) Fiore, M.; Magi, V.; Viggiano, A. Internal combustion engines powered by syngas: A review. *Appl. Energy* **2020**, *276*, No. 115415.
(11) Dai, X.; Ji, C.; Wang, S.; Liang, C.; Liu, X.; Ju, B. Effect of syngas addition on performance of a spark-ignited gasoline engine at lean conditions. *Int. J. Hydrogen Energy* **2012**, *37*, 14624−14631.
(12) Ji, C.; Dai, X.; Wang, S.; Liang, C.; Ju, B.; Liu, X. Experimental study on combustion and emissions performance of a hybrid syngas−gasoline engine. *Int. J. Hydrogen Energy* **2013**, *38*, 11169−11173.
(13) Singh, H.; Mohapatra, S. K. Production of producer gas from sugarcane bagasse and carpentry waste and its sustainable use in a dual fuel CI engine: A performance, emission, and noise investigation. *J. Energy Inst.* **2018**, *91*, 43−54.
(14) Krishnamoorthi, M.; Sreedhara, S.; Prakash Duvvuri, P. Experimental, numerical and exergy analyses of a dual fuel combustion engine fuelled with syngas and biodiesel/diesel blends. *Appl. Energy* **2020**, *263*, No. 114643.
(15) Xu, Z.; Jia, M.; Xu, G.; Li, Y.; Zhao, L.; Xu, L.; Lu, X. Potential for Reducing Emissions in Reactivity-Controlled Compression Ignition Engines by Fueling Syngas and Diesel. *Energy Fuels* **2018**, *32*, 3869−3882.
(16) Xu, Z.; Jia, M.; Li, Y.; Chang, Y.; Xu, G.; Xu, L.; Lu, X. Computational optimization of fuel supply, syngas composition, and intake conditions for a syngas/diesel RCCI engine. *Fuel* **2018**, *234*, 120−134.
(17) Jain, S.; Li, D.; Aggarwal, S. K. Effect of hydrogen and syngas addition on the ignition of iso-octane/air mixtures. *Int. J. Hydrogen Energy* **2013**, *38*, 4163−4176.
(18) Kongsereeparp, P.; Checkel, M. D. *Study of Reformer Gas Effects on n-Heptane HCCI Combustion Using a Chemical Kinetic Mechanism Optimized by Genetic Algorithm*; SAE International, 2008.
(19) Neshat, E.; Saray, R. K.; Parsa, S. Numerical analysis of the effects of reformer gas on supercharged n-heptane HCCI combustion. *Fuel* **2017**, *200*, 488−498.
(20) Azimov, U.; Okuno, M.; Tsuboi, K.; Kawahara, N.; Tomita, E. Multidimensional CFD simulation of syngas combustion in a micro-pilot-ignited dual-fuel engine using a constructed chemical kinetics mechanism. *Int. J. Hydrogen Energy* **2011**, *36*, 13793−13807.
(21) Ra, Y.; Chuahy, F.; Kokjohn, S. Development and validation of a reduced reaction mechanism with a focus on diesel fuel/syngas co-oxidation. *Fuel* **2016**, *185*, 663−683.
(22) Kozlov, V. E.; Titova, N. S.; Chechet, I. V. Modeling study of hydrogen or syngas addition on combustion and emission characteristics of HCCI engine operating on iso-octane. *Fuel* **2018**, *221*, 61−71.
(23) Neshat, E.; Saray, R. K.; Hosseini, V. Investigation of the effect of reformer gas on PRFs HCCI combustion based on exergy analysis. *Int. J. Hydrogen Energy* **2016**, *41*, 4278−4295.
(24) Neshat, E.; Saray, R. K.; Hosseini, V. Effect of reformer gas blending on homogeneous charge compression ignition combustion of primary reference fuels using multi zone model and semi detailed chemical-kinetic mechanism. *Appl. Energy* **2016**, *179*, 463−478.
(25) Reyhanian, M.; Hosseini, V. Various effects of reformer gas enrichment on natural-gas, iso-octane and normal-heptane HCCI combustion using artificial inert species method. *Energy Convers. Manage.* **2018**, *159*, 7−19.
(26) Khan, F.; Elbaz, A. M.; Badra, J.; Costanzo, V.; Roberts, W. L. A Comprehensive Experimental and Kinetic Study of Laminar Flame Characteristics of H2 and CO Addition to Oxygenated Gasoline. *Energy Fuels* **2021**, *35*, 14063−14076.
(27) Pio, G.; Wako, F. M.; Salzano, E. On the prediction of the ignition delay time of bio-syngas. *Chem. Eng. Trans.* **2020**, *82*, 271−276.
(28) Davis, S. G.; Joshi, A. V.; Wang, H.; Egolfopoulos, F. An optimized kinetic model of H2/CO combustion. *Proc. Combust. Inst.* **2005**, *30*, 1283−1292.
(29) Kéromnès, A.; Metcalfe, W. K.; Heufer, K. A.; Donohoe, N.; Das, A. K.; Sung, C.-J.; Herzler, J.; Naumann, C.; Griebel, P.; Mathieu, O.; Krejci, M. C.; Petersen, E. L.; Pitz, W. J.; Curran, H. J. An experimental and detailed chemical kinetic modeling study of hydrogen and syngas mixture oxidation at elevated pressures. *Combust. Flame* **2013**, *160*, 995−1011.
(30) Li, J.; Zhao, Z.; Kazakov, A.; Chaos, M.; Dryer, F. L.; Scire, J. J., Jr. A comprehensive kinetic mechanism for CO, CH2O, and CH3OH combustion. *Int. J. Chem. Kinet.* **2007**, *39*, 109−136.
(31) Kalitan, D.; Petersen, E. Ignition and Oxidation of Lean CO/H2 Fuel Blends in Air. *J. Propul. Power* **2007**, *23*, 1291−1301.
(32) Sun, H.; Yang, S. I.; Jomaas, G.; Law, C. K. High-pressure laminar flame speeds and kinetic modeling of carbon monoxide/hydrogen combustion. *Proc. Combust. Inst.* **2007**, *31*, 439−446.
(33) Frassoldati, A.; Faravelli, T.; Ranzi, E. The ignition, combustion and flame structure of carbon monoxide/hydrogen mixtures. Note 1: Detailed kinetic modeling of syngas combustion also in presence of nitrogen compounds. *Int. J. Hydrogen Energy* **2007**, *32*, 3471−3485.
(34) Mehl, M.; Pitz, W. J.; Westbrook, C. K.; Curran, H. J. Kinetic modeling of gasoline surrogate components and mixtures under engine conditions. *Proc. Combust. Inst.* **2011**, *33*, 193−200.
(35) Cancino, L. R.; Fikri, M.; Oliveira, A. A. M.; Schulz, C. Autoignition of gasoline surrogate mixtures at intermediate temperatures and high pressures: Experimental and numerical approaches. *Proc. Combust. Inst.* **2009**, *32*, 501−508.
(36) Zhao, Z.; Conley, J.; Kazakov, A. F.; Dryer, F. L., *Burning Velocities of Real Gasoline Fuel at 353 K and 500 K*. 2003; *112*, 2624−2629.
(37) Huang, Y.; Sung, C. J.; Eng, J. A. Laminar flame speeds of primary reference fuels and reformer gas mixtures. *Combust. Flame* **2004**, *139*, 239−251.
(38) Jerzembeck, S.; Peters, N.; Pepiot-Desjardins, P.; Pitsch, H. Laminar burning velocities at high pressure for primary reference fuels and gasoline: Experimental and numerical investigation. *Combust. Flame* **2009**, *156*, 292−301.
(39) Kelley, A. P.; Smallbone, A. J.; Zhu, D. L.; Law, C. K. Laminar flame speeds of C5 to C8 n-alkanes at elevated pressures: Experimental determination, fuel similarity, and stretch sensitivity. *Proc. Combust. Inst.* **2011**, *33*, 963−970.

https://doi.org/10.1021/acsomega.2c06515
ACS Omega 2023, 8, 3929−3944